FORMING PARAMETERS MULTI-OBJECTIVE OPTIMIZATION AND MOLD DESIGN OF VEHICLE REINFORCEMENT PLATE TYPE WORKPIECES

Haibo ZHANG[1], Tianwu WANG[2]

Taking the left/right gas spring reinforcement plate of a certain model of electric vehicle rear door as the research object, the structure characteristics and forming requirements of the key deformation area on the surface were analyzed, and the key stamping process was designed with AutoForm software. Taking the maximum thickening rate and the maximum spring back as the optimization indicators, the orthogonal test of 5 factors and 4 levels was designed with the blank holder force, friction coefficient, draw bead resistance coefficient, stamping speed, convex and concave mold gap as the parameter variables. Through the comparison of gray correlation theory and the range analysis method, the parameter combination with the best comprehensive forming quality was obtained. On this basis, the die design was guided to complete, and qualified parts with good quality were obtained through numerical simulation and mold trial verification, which has guiding significance for the processing and production of similar stamping parts.

Keywords: gas spring reinforcement plate; stamping forming; orthogonal test; gray correlation theory; multi-objective optimization; mold design.

1. Introduction

In the process of vehicle design and manufacturing, body panels are the most intuitive part of vehicle parts, and their quality is one of the important factors that affect the core competitiveness of vehicles. The most fundamental purpose of reinforcement plate type workpieces is to ensure that the main parts have sufficient rigidity, strength, and connection stability. However, when the process parameters are not selected properly, defects such as scratches, cracks, and wrinkles will appear on the surface of the part. These defects seriously affect the forming quality, assembly accuracy, and mechanical properties of the product, and there is a certain coupling relationship between different forming defect evaluation indexes. Experience alone cannot minimize all defect indicators at the same time[1-2]. The

[1] Engineering Training and Teaching Center, Northeast Electric Power University, Jilin City, Jilin Province, China, 132012, e-mail: 1506604443@qq.com

[2] School of Mechanical Engineering, Northeast Electric Power University, Jilin City, Jilin Province, China, 132012, e-mail: wangtianwu0609@163.com

optimization of traditional stamping process parameters is an extension of the classic "trial and error", which needs to be continuously tested and debugged in combination with actual production experience. Nowadays, the sheet metal forming numerical simulation technology with the finite element method as the core provides a more convenient and effective research method for the stamping process design and mold cavity optimization of vehicle panels[3-4].

Wang H applied the method of combining the least square support vector machine and a parallel learning strategy to optimize the forming force distribution in each area of the sheet metal forming process[5]. Sun G Y used the 6sigma robust optimization design method in quality engineering to establish a response surface model between process parameters and rupture and wrinkling evaluation functions. The particle swarm optimization algorithm was applied to parameter design, the practicability and accuracy of parameter optimization were proved by calling the surrogate model.[6]. Long L established a support vector machine model with the maximum thickening rate and maximum thinning rate as evaluation indicators, and used a random focus search algorithm and penalty function to select the optimal process parameters[7]. Kahhal P used a genetic algorithm and the response surface method to establish a proxy model between forming parameters and forming quality defects of cross-shaped parts, and obtained a Pareto set for optimization of process parameters[8]. Manoochehri applied a neural network and simulated annealing to deep drawing simulation, and optimized parameters such as mold fillet radius, friction coefficient, blank holder force and so on[9]. Yang X J introduced adaptive mutation particles, dynamic acceleration factors and dynamic inertia weights into the standard particle swarm algorithm. By improving the particle swarm algorithm to optimize the forming process parameters, the forming quality of the workpiece was effectively improved[10].

The multi-objective optimization of stamping process parameters can effectively adjust the flow velocity and stress-strain relationship of the blank metal in various places during the forming process, thereby reducing or eliminating forming quality defects and realizing control of the stamping process[11]. This paper took a certain type of electric vehicle rear door gas spring reinforcement plate as the research object, and designed the key process of stamping through parts analysis. On the basis of the orthogonal test, the sheet metal forming parameter optimization technology based on gray correlation theory was used to construct the mapping relationship between each parameter and the multi-objective optimization under the premise of the known partial quantitative simulation parameters, so as to obtain the best forming parameter scheme. According to the optimized parameter scheme, the mold is designed, and a well-formed qualified part is obtained. This method not only shortens the parameter debugging time, but also effectively solves defects such as excessive thinning, edge tearing, and shape changes. It has important reference

significance and practical value for the quality assurance and follow-up production of reinforcement plate-type workpieces.

2. Workpiece Analysis

The vehicle rear door gas spring reinforcement plate is symmetrical, mainly composed of convex and concave curved surfaces. The workpiece has many transition arcs and large cross-section changes. The lap joints on both sides have an expanded flange shape, and the flange part is difficult to form. The whole presents a support plate structure with a complicated stepped shape. Its surface has multiple grooves for connection directions and process holes of different sizes, and the workpiece presents various inclined plane shapes. The three-dimensional model is shown in Figure 1. The product is formed in pairs at the same time. The material is ST280 cold-rolled steel with a thickness of 1.6mm. The main material performance parameters are shown in Table 1.

Table 1

Main parameters of ST280 material performance

Physical quantity	Numerical value
Yield Strength(R_{eL}/MPa)	313.8
Tensile strength(R_m/MPa)	477.5
Hardening Index(n)	0.156
Thickness anisotropy coefficient(V_r)	1.17
Poisson's ratio(μ)	0.3

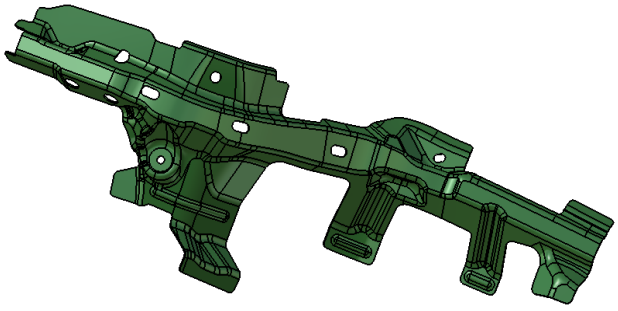

Fig. 1. Three-dimensional model of gas spring reinforcement plate

3. Numerical Simulation

3.1 Modeling

This paper used AutoForm software to import the three-dimensional model of the vehicle rear door gas spring reinforcement plate, adopted the adaptive function to divide the mesh. Set the mesh tolerance to 0.1mm and the longest side length to be 30mm. The mesh size of the area with large local deformation would

automatically become smaller[12]. The shape material is selected for processing, and the material size is 1380mm × 310mm. The workpiece adopted the equivalent virtual drawbead, selected the appropriate stamping direction under the premise of no negative stamping angle, and tried to make the contact position between the blank metal and the mold in the center of the mold[13]. Most of the shape of this workpiece was realized by reshaping, so there were relatively few process supplements, mainly including hole sealing, flange flattening, gap filling and blank holder design. Among them, the boundary line was used as the reference line to set the conformal blank holder, focusing on the controllability of material flow and the advantage of forming[14]. In this paper, the finite element model of the drawing forming of the gas spring reinforcement plate is established as shown in Figure 2.

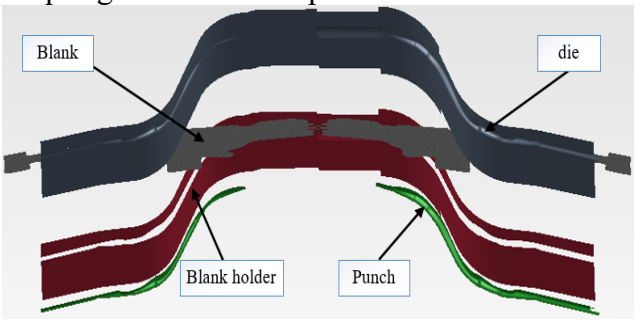

Fig. 2. Finite Element Model of Gas Spring Reinforcement Plate

3.2 First Simulation

The reinforcement plate is mainly used to strengthen the connection between parts and play a certain curing effect. Because the drawing depth of this workpiece is relatively shallow, according to the production experience of similar products, the overall maximum thinning rate should not exceed 30% and the maximum thickening rate should not exceed 20% after all forming[15]. There is no rigid requirement for wrinkling after all forming, and the springback is minimized as much as possible[16]. The preliminary selection process parameters of this workpiece are blank holder force of 500kN, friction coefficient of 0.13, drawbead resistance coefficient of 0.3, stamping speed of 600mm/s, convex and concave mold gap of 1.6mm. Using AutoForm software to carry out the numerical simulation of stamping forming, the sheet metal thickness cloud diagram and springback simulation results are shown in Figure 3 (a) and (b) respectively. It can be seen from Figure 3 that most areas of the part are well-formed, with a maximum thinning rate of 22.2%, but a maximum thickening rate of 20.1%, there are forming defects with serious thickening in the critical control area. The maximum springback of this part is 1.726 mm, and the springback in the local area is too large, so the initial parameters need to be optimized.

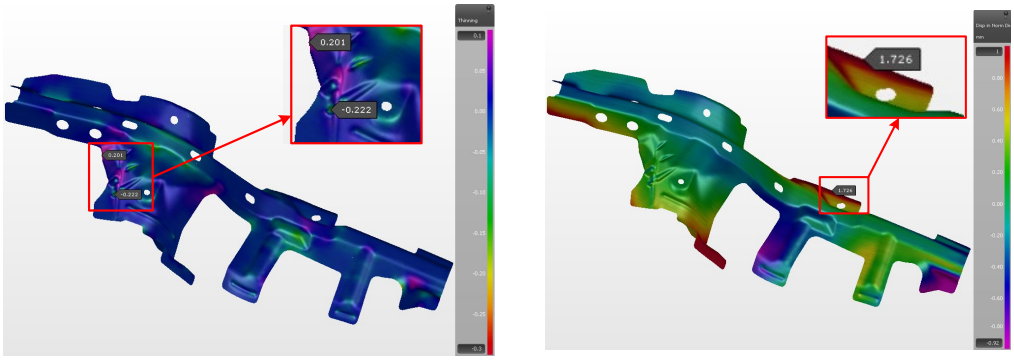

(a) Sheet metal thickness cloud diagram (b) Springback simulation results

Fig. 3. Sheet metal forming simulation results under initial data

4. Multi-objective Optimization

4.1 Orthogonal Design

The orthogonal test selects samples to be scattered, neat and uniform, and the overall law can be reflected through representative tests. It is an efficient experimental design method for seeking the best level combination of multiple factors. This paper selects the five factors as the self-variable that has the greatest impact on the forming quality of the workpiece. They are blank holder force (*A*), friction coefficient (*B*), drawbead resistance coefficient (*C*), stamping speed (*D*), convex and concave mold gap (*E*). Four levels are selected for each factor, and an orthogonal table is established using the $L_{16}(4^5)$ standard. The levels of orthogonal test factors are shown in Table 2. AutoForm software was applied to carry out 16 stamping simulation simulations, and the test results are shown in Table 3. It can be seen from Table 3 that the maximum thinning rate of the 16 sets of workpiece forming simulation results is less than 30%, so the maximum thickening rate and the maximum springback are selected as the optimization indicators.

Table 2

Orthogonal test factor level table

Level	Factor				
	A/kN	B	C	D/mm•s^{-1}	E/mm
1	500	0.12	0.25	500	1.4
2	700	0.14	0.35	1000	1.5
3	900	0.16	0.45	1500	1.6
4	1100	0.18	0.55	2000	1.7

Table 3

Orthogonal test results

Test number	Test factors					Simulation results		
	A(*kN*)	B	C	D(*mm/s*)	E(*mm*)	Maximum springback $Y_1(mm)$	Maximum thickening rate $Y_2(\%)$	Maximum thinning rate $Y_3(\%)$
1	500	0.12	0.25	500	1.4	1.637	13.1	21.9
2	500	0.14	0.35	1000	1.5	1.516	14.9	19.5
3	500	0.16	0.45	1500	1.6	1.571	22.2	18.7
4	500	0.18	0.55	2000	1.7	1.267	15.6	19.8
5	700	0.12	0.35	1500	1.7	1.728	12.4	22.3
6	700	0.14	0.25	2000	1.6	1.381	18.7	15.8
7	700	0.16	0.55	500	1.5	1.437	22.7	17.6
8	700	0.18	0.45	1000	1.4	1.420	16.5	20.7
9	900	0.12	0.45	2000	1.5	1.645	13.4	16.5
10	900	0.14	0.55	1500	1.4	1.554	17.5	19.2
11	900	0.16	0.25	1000	1.7	1.643	16.7	16.2
12	900	0.18	0.35	500	1.6	1.556	14.2	21.4
13	1100	0.12	0.55	1000	1.6	1.732	18.2	22.7
14	1100	0.14	0.45	500	1.7	1.701	20.1	16.3
15	1100	0.16	0.35	2000	1.4	1.638	17.8	17.4
16	1100	0.18	0.25	1500	1.5	1.426	14.3	17.7

4.2 Range Analysis

The difference between the maximum value and the minimum value of the average index of the test results for any factor at each level is called the range of the factor. The specific calculation formula of the range analysis method is as follows.

$$\begin{cases} k_{ij} = \overline{\sum K_{ij}} \\ R = k_{\max} - k_{\min} \end{cases} \tag{1}$$

Among them, i represents each factor, j represents each level, and R is the extreme range result corresponding to each factor. Calculate 16 sets of simulation results according to the above formula. When the maximum springback is used as the optimization index, the range analysis of the test results is shown in Table 4. When the maximum thickening rate is used as the optimization index, the range analysis of the test results is shown in Table 5.

Table 4

Range analysis of maximum springback test results

Level	A	B	C	D	E
Mean(k_1)	1.49775	1.68550	1.52175	1.58275	1.56225
Mean(k_2)	1.49150	1.53800	1.60950	1.57775	1.50600
Mean(k_3)	1.59950	1.57225	1.58425	1.56975	1.56000
Mean(k_4)	1.62425	1.41725	1.49750	1.48275	1.58475
Range value(R)	0.13275	0.26825	0.11200	0.10000	0.07875

Table 5

Range analysis of maximum thickening rate test results

Level	A	B	C	D	E
Mean(k_1)	16.450	14.275	15.700	17.525	16.225
Mean(k_2)	17.575	17.800	14.825	16.575	16.325
Mean(k_3)	15.450	19.850	18.050	16.600	18.325
Mean(k_4)	17.600	15.150	18.500	16.375	16.200
Range value(R)	2.150	5.575	3.675	1.150	2.125

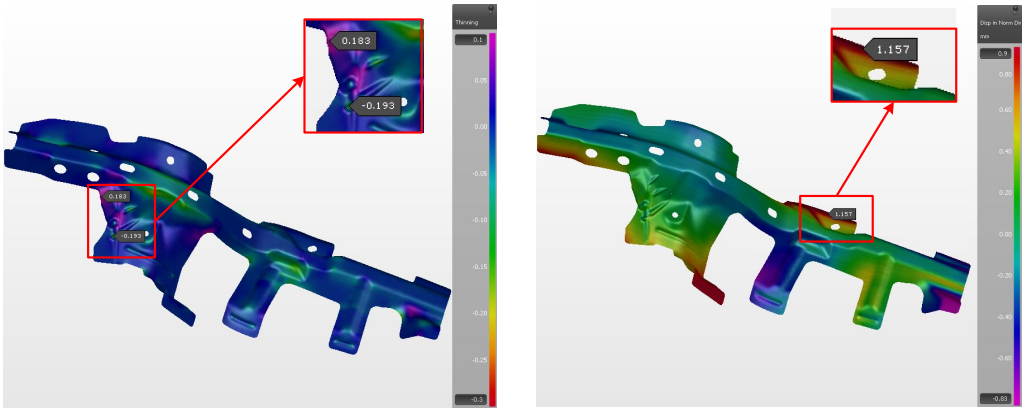

(a) Sheet metal thickness cloud diagram (b) Springback simulation results

Fig. 4. Simulation results of sheet metal forming under single-objective optimization of maximum springback

It can be seen from Table 4 that for the maximum springback, the order of influence of various factors on the formability of the part is: *B>A>C>D>E*. At this time, the optimal horizontal combination of process parameters is *A2B4C4D4E2*, that is, blank holder force of 700kN, friction coefficient of 0.18, drawbead resistance coefficient of 0.55, stamping speed of 2000mm/s, convex and concave mold gap of 1.5mm. Under this parameter optimization scheme, the sheet metal thickness cloud diagram and the springback simulation results are shown in Figure 4 (a) and (b) respectively. It can be seen from Figure 4 that the maximum thinning rate of part forming is 19.3%, which meets the production requirements. The

maximum springback is 1.157mm, which is smaller than any set of test springbacks in the orthogonal table, but the maximum thickening rate is 18.3%, which has approached the limit value, which has a certain impact on the assembly accuracy.

It can be seen from Table 5 that for the maximum thickening rate, the order of influence of various factors on the formability of the part is: *B*>*C*>*A*>*E*>*D*. At this time, the optimal horizontal combination of process parameters is *A3B1C2D4E4*, that is, blank holder force of 900kN, friction coefficient of 0.12, drawbead resistance coefficient of 0.35, stamping speed of 2000mm/s, convex and concave mold gap of 1.7mm. Under this parameter optimization scheme, the sheet metal thickness cloud diagram and the springback simulation results are shown in Figure 5 (a) and (b) respectively. It can be seen from Figure 5 that the maximum thinning rate of part forming is 19.7%, which meets the production requirements. The maximum thickening rate is 11.4%, which is smaller than any set of test thickening rates in the orthogonal table, but the maximum springback is 1.693mm, which still needs to be further optimized for subsequent springback compensation.

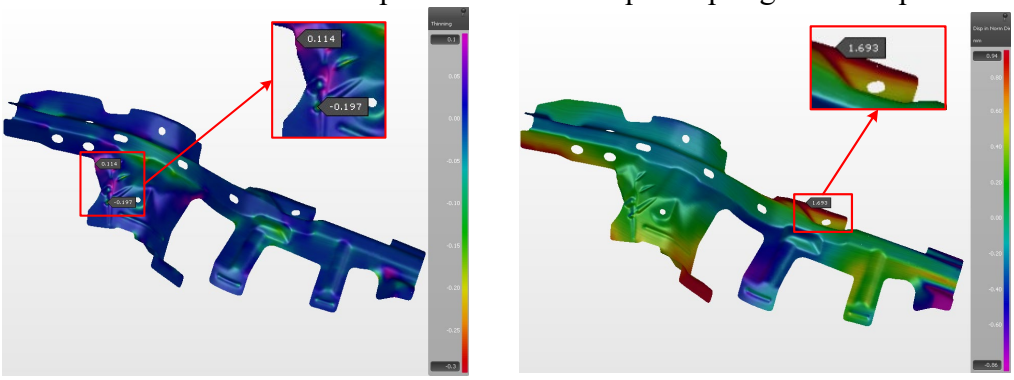

(a) Sheet metal thickness cloud diagram (b) Springback simulation results

Fig. 5. Simulation results of sheet metal forming under single-objective optimization of maximum thickening rate

Therefore, only relying on the range analysis method can not simultaneously reduce the thickening and springback defects to the minimum. This paper uses the grey relational theory to transform multi-objective optimization into a unified process, and then obtains the optimal parameter combination that takes into account the two optimization indexes to improve the comprehensive forming quality of the gas spring reinforcement plate.

4.3 Grey Relational Analysis

Grey relational theory is an analysis method that uses known information to predict unknown information and understand the overall development trend of the system. It mainly measures the degree of connection between the influencing factors and the optimization goal by calculating the gray correlation degree[17]. The greater the gray correlation degree of each factor at the corresponding parameter level, the greater its response to the optimization target, and the better the stamping

effect of the part. Because the optimization goals have different meanings and the dimensions of each parameter are different, the threshold method is used to perform dimensionless processing on the 16 groups of original data. The calculation formula is shown in equation (2), where $x(k)$ is the original data and $y(k)$ is the processed data.

$$y(k)=\frac{x(k)-\min\limits_{k\in n}x(k)}{\max\limits_{k\in n}x(k)-\min\limits_{k\in n}x(k)} \tag{2}$$

According to the analysis method of gray correlation theory, the minimum value of the maximum thickening rate and maximum springback of the workpiece forming in the orthogonal experiment is selected as the reference sequence, which is recorded as $Y_0=\{12.4,\ 1.267\}$. Then calculate the absolute difference of the corresponding elements of the 16 sets of reference sequences and comparison sequences, and solve the gray correlation coefficient between each factor and the single objective. Finally, the gray correlation coefficient is used to solve the weighted average to obtain the correlation degree between each factor and multiple objectives. The calculation formula of the gray correlation coefficient is shown in equation (3), and the calculation formula of gray correlation degree is shown in equation (4).

$$\xi_i(k)=\frac{\min\limits_i\min\limits_k\left|x_0(k)-x_i(k)\right|+\rho\max\limits_i\max\limits_k\left|x_0(k)-x_i(k)\right|}{\left|x_0(k)-x_i(k)\right|+\rho\max\limits_i\max\limits_k\left|x_0(k)-x_i(k)\right|} \tag{3}$$

$$r(x_0,x_i)=\frac{1}{n}\sum\nolimits_{k=1}^{n}\lambda_k\xi_i(k) \tag{4}$$

In formula (3), ρ is the resolution coefficient, usually ρ=0.5 in order to observe changes in the degree of correlation. In formula (4), λ_k is the weight, and the weight of the maximum thickening rate and the maximum springback amount is equal, that is, $\lambda_1=\lambda_2=0.5$. After calculation, the gray correlation coefficient and gray correlation degree of the 16 groups of experimental data and the objective function are shown in Table 6, and the average correlation degree of each factor to the optimization indicator at different levels is shown in Table 7.

Table 6

The gray correlation coefficient and gray correlation degree of 16 sets of experimental data and the objective function

Test number	Grey correlation coefficient(ξ_1)	Grey correlation coefficient(ξ_2)	Grey relational degree(r)
1	0.386	0.880	0.633
2	0.483	0.673	0.578
3	0.433	0.345	0.389
4	1.000	0.617	0.809

5	0.335	1.000	0.668
6	0.671	0.450	0.561
7	0.577	0.333	0.455
8	0.603	0.557	0.580
9	0.381	0.838	0.610
10	0.448	0.503	0.476
11	0.382	0.545	0.464
12	0.446	0.741	0.594
13	0.333	0.470	0.402
14	0.349	0.401	0.375
15	0.385	0.488	0.437
16	0.594	0.731	0.663

Table 7

The average correlation degree of each factor to the optimization index

Level	A	B	C	D	E
Mean(k_1)	0.60225	0.57825	0.58025	0.51425	0.5315
Mean(k_2)	0.56600	0.49750	0.56925	0.50600	0.5765
Mean(k_3)	0.53600	0.43625	0.48850	0.54900	0.4865
Mean(k_4)	0.46925	0.66150	0.53550	0.60425	0.5790
Range value(R)	0.13300	0.22525	0.09175	0.09825	0.09250

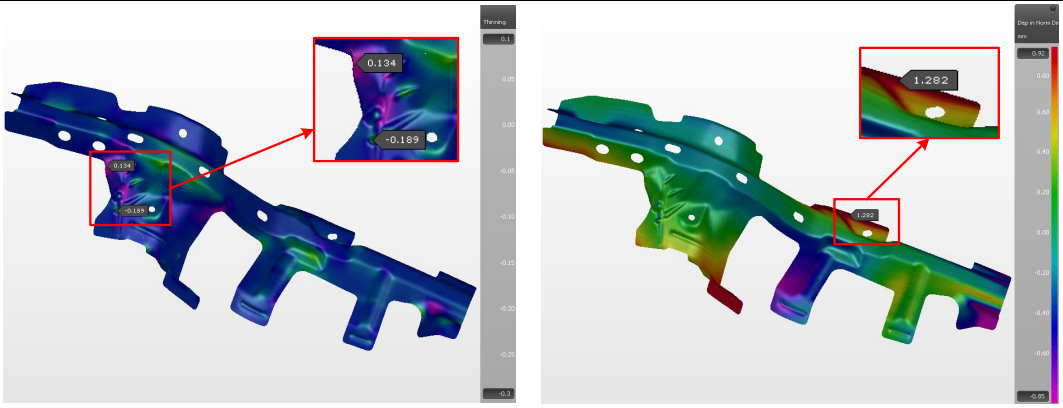

(a) Sheet metal thickness cloud diagram (b) Springback simulation results

Fig. 6. Simulation results of sheet metal forming under multi-objective optimization of maximum thickening rate and maximum springback

When using the gray correlation theory to optimize the parameter scheme, the larger the average correlation degree value of a certain independent variable to the optimization index is, the closer the corresponding result of the independent variable is to the optimal solution. It can be seen from Table 7 that when the

maximum thickening rate and the maximum springback amount are used as the comprehensive optimization indicators, the order of influence of each factor on the gray correlation of the optimization objective is: *B>A>D>E>C*. The horizontal combination of process parameters with the largest gray correlation is *A1B4C1D4E4*, that is, blank holder force of 500kN, friction coefficient of 0.18, drawbead resistance coefficient of 0.25, stamping speed of 2000mm/s, convex and concave mold gap of 1.7mm. Under this parameter optimization scheme, the sheet metal thickness cloud diagram and the springback simulation results are shown in Figure 6 (a) and (b) respectively. It can be seen from Figure 6 that the maximum thinning rate of the part forming is 18.9%, the maximum thickening rate is 13.4%, and the maximum springback is 1.282mm. There are no quality defects in the key areas and the comprehensive forming effect is the best.

5. Debug Mold

5.1 Mold Development

The workpiece has many free-form surfaces and diverse connection changes. After the main body is processed into a curved shape, it needs to be combined with reshaping correction to ensure that each branch plate structure is shaped as required. In order to improve product quality and stamping accuracy, a single-process mold and a composite mold were selected for the stamping mold of this workpiece, and a total of three reshape processes were introduced. The stamping process scheme of the gas spring reinforcement plate was determined as follows: draw → pierce, side pierce → restrike → flanging restrike → restrike, side restrike → pierce, side pierce.

5.1.1 Drawing Mold Design

In this paper, the drawing die surface is derived from the AutoForm software, and the drawing mold is designed with a single-action drawing inverted structure. In order to avoid quality defects such as napping, the punch and the lower mold base are cast separately and connected to each other by bolts. The punch is a shell structure, located in the center of the press, and the outline size is set as the product surface size. Each part of the mold should be guided by guide plates. Set the positioning pins according to the vertical sheet metal line and the principle of closed positioning. The lifting device adopts the cast-in hanging rod, and the material pressing core is designed based on the outer contour of the drawing mold surface[18].

The total pressure of the drawing mold press is mainly selected according to the sum of drawing force and blank holder force. The drawing force calculation formula is shown in equation (5). In order to avoid the overload and damage of the press due to the premature occurrence of the maximum stamping force, the standard pressure of the press in the case of shallow drawing is generally estimated according to formula (6).

$$F = KLtR_m \tag{5}$$

$$F_Z \leq (0.7 \sim 0.8)\ F_0 \tag{6}$$

In formula (5), K is the correction factor, usually K=0.8, L is the perimeter of the punch, t is the thickness of the sheet, and R_m is the tensile strength of the material. In formula (6), F_Z is the total deformation force, and F_0 is the standard pressure of the press. According to formula (5), the drawing force is estimated to be about 3700kN. Since the blank holder force is selected as 500kN in the multi-objective optimization parameter scheme, a 6000kN press is initially selected according to formula (6). The punch structure of the drawing mold of this workpiece is shown in Figure 7.

5.1.2 Reshaping Mold Design

The workpiece is reshaped mainly by the reshaping insert contacting the sheet material, in which the arc part is made into a single piece and fastened by screws. The reshaping mold still adopts the pressing core device, which uses the pressing core guide plate to contact the inner and outer sidewalls of the cavity to guide the slide and realize the mold stroke control. The pressing core device relies on the safety bolt to limit the movement, and the working direction of the safety bolt is consistent with the stamping direction to ensure the stroke control of the pressing core. A nitrogen gas spring is used as an elastic element to be fixedly installed at the bottom of the upper mold base, and acts on the pressing core to provide pressing force during the downward movement of the press. When side reshaping, press the material along the normal direction of the area with a smaller forming angle, and at the same time, the pressing plate presses the formed part to prevent secondary deformation. When flanging, the fillet radius of the die is equal to the fillet radius of the workpiece, and the fillet radius of the punch is set to about 4 times the plate thickness to improve the plastic flow conditions of the plate[19]. In addition, work hardening occurs in the bulging of the sheet metal in the reshaping area, which improves the rigidity of the area to a certain extent and effectively controls the springback problem[20]. The three-time reshaping punch structure of this workpiece is shown in Figures 8, 9, and 10.

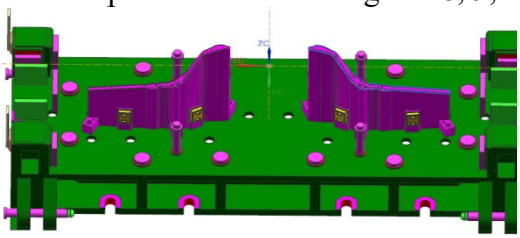

Fig. 7. OP10 Drawing mold punch

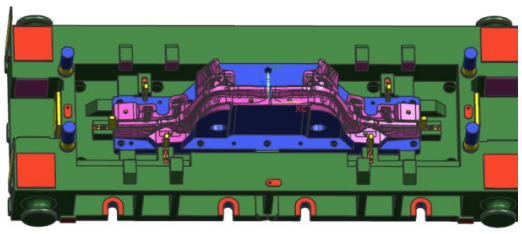

Fig. 8. OP30 Reshaping mold punch

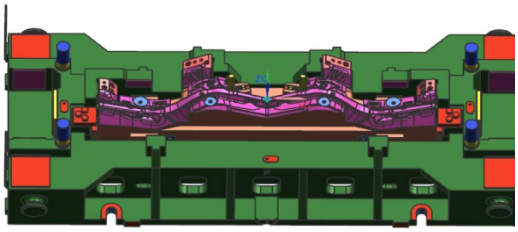

Fig. 9. OP40 Flanging and reshaping mold punch

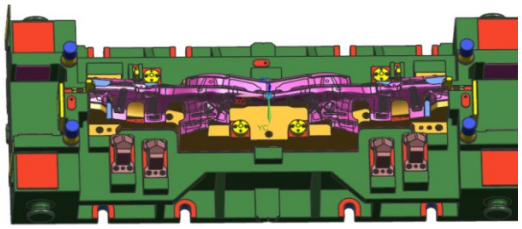

Fig. 10. OP50 Reshaping and side reshaping mold punch

5.2 Production Test

Under the premise of ensuring tolerance requirements, a multi-objective optimization parameter scheme was used to guide mold assembly and debugging. Springback control was performed through the optimization of the die surface to prevent the pressing device of the next process from contacting the surface of the rebound state of the previous process, thereby causing surface damage. After actual production, the part was fully formed without quality defects, and the maximum thinning rate, maximum thickening rate and maximum springback were basically consistent with the finite element simulation results. We randomly picked a number of points on the actual production objects for three-coordinate size measurement, and the measured values were basically consistent with the simulated values. The final product of the vehicle rear door reinforcement plate produced by the production and assembly of the gas spring reinforcement plate and the hinge reinforcement plate is shown in Figure 11. The stiffness method was used to detect the stiffness of the product, and the test result was qualified and met the assembly requirements.

Fig. 11. This model of electric vehicle rear door reinforcement plate assembly product

6. Conclusion

(1) According to the structural characteristics of the vehicle rear door gas spring reinforcement plate, the key stamping process design, including blanking surface design, stamping direction selection, and process supplement surface optimization, is carried out on it. AutoForm software was used to establish a finite element model of sheet metal forming, and a 5-factor 4-level orthogonal test was designed with blank holder force, friction coefficient, drawbead resistance coefficient, stamping speed, convex and concave mold gap as independent variables.

(2) Parameter optimization is carried out by the range analysis method. When the maximum springback is the optimization target, the maximum springback of sheet metal forming under the optimal parameter combination is 1.157mm, which is smaller than any set of test springbacks, but the maximum thickening rate is 18.3%, which has approached the limit value. When the maximum thickening rate is the optimization target, the maximum thickening rate of sheet metal forming under the optimal parameter combination is 11.4%, which is smaller than any set of test thickening rates, but the maximum springback is 1.693mm, which needs to be further optimization.

(3) Multi-objective optimization of parameters is carried out by grey relational theory. Taking the maximum thickening rate and the maximum springback as the evaluation index, the optimal parameter combination is the blank holder force of 500kN, the friction coefficient of 0.18, the drawbead resistance coefficient of 0.25, the stamping speed of 2000mm/s, and the convex and concave mold gap of 1.7mm. Under the scheme, the maximum thickening rate of sheet metal forming is 13.4%, the maximum springback is 1.282mm, and the comprehensive forming effect is the best.

(4) To ensure that the parts are fully formed, a total of three reshape processes are introduced. The stamping process scheme of the gas spring reinforcement plate is determined as follows: draw → pierce, side pierce → restrike → flanging restrike → restrike, side restrike → pierce, side pierce. Guide the mold design according to the optimized parameter scheme. Through numerical simulation and mold trial verification, qualified parts with good quality have been obtained, which proves that orthogonal tests combined with gray correlation theory can effectively carry out multi-objective optimization of forming parameters. This has a certain reference value for improving the production efficiency of parts and the processing and production of similar stamping parts.

REFERENCES

[1] *Moghadam Marcel, Chris Valentin, Bay Niels*, "Analysis of the risk of galling in sheet metal stamping dies with drawbeads," Proceedings of the Institution of Mechanical Engineers, **vol. 234**, no. 9, Jul. 2020, pp. 1207-1214

[2] *Gu Zhengwei, Li Shizhong, Zhao Lihui, Zhu Lijuan, Yu Ge*, "Finite element simulation and experimental investigations of cold stamping forming defect of A588-A thick weathering steel bogie lower cover," International Journal of Advanced Manufacturing Technology, **vol. 104**, no. 1-4, Sep. 2009, pp. 1275-1283

[3] *Isazadeh Amir Reza, Shamloofard Mansoor, Assempour Ahmad*, "Some improvements on the one-step inverse isogeometric analysis by proposing a multi-step inverse isogeometric methodology in sheet metal stamping processes," Applied Mathematical Modelling, **vol. 91**, no. 2, Mar. 2021, pp. 476-492

[4] *Sudarsan Coomar, Sajun Prasad, Hazra Sumit, Sushanta Kumar* "Forming of serpentine micro-channels on SS304 and AA1050 ultra-thin metallic sheets using stamping technology," Journal of Manufacturing Processes, **vol. 56**, no. 2, Aug. 2020, pp. 1099-1113

[5] *Wang Hu, Li Enying, Li Guang Yao*, "The least square support vector regression coupled with parallel sampling scheme metamodeling technique and application in sheet forming optimization," Materials & Design, **vol. 30**, no. 5, Aug. 2008, pp. 1468-1479

[6] *Sun Guangyong, Li Guangyao, Chen Tao*, "Application of multi-objective particle swarm optimization algorithm in sheet metal forming," Journal of Mechanical Engineering, **vol. 45**, no. 5, May. 2009, pp. 153-159

[7] *Long Ling, Yin Guofu, Zou Yun*, "Stamping process optimization based on random focus search algorithm," Computer Integrated Manufacturing Systems, **vol. 18**, no. 2, Feb. 2012, pp. 314-320

[8] *Kahhal P, Azodi H D*, "Multi-objective Optimization of Sheet Metal Forming Die Using Genetic Algorithm Coupled with RSM and FEA," Journal of Failure Analysis & Prevention, **vol. 13**, no. 6, Dec. 2013, pp. 771-778

[9] *Manoochehri, Mohsen*, "Integration of artificial neural network and simulated annealing algorithm to optimize deep drawing process," International Journal of Advanced Manufacturing Technology, **vol. 73**, no. 1-4, Jul. 2014, pp. 241-249

[10] *Yang Xujing, Feng Xiaolong, Zheng Juan*, "Application of SVM and improved particle swarm algorithm in the optimization of stamping forming," Automotive Engineering, **vol. 37**, no. 4, Apr. 2015, pp. 485-489

[11] *Su C.J. , Dong X.H. , Wang Q. , Mu Y.D.* , "Study on the effects of forming parameters on the plastic flow of axisymmetrical curved parts in stamping process," Materials Research Innovations, **vol. 19**, no. 2, Nov. 2015, pp. 359–364

[12] *Shamloofard Mansoor, Assempour Ahmad*, "Simulation of sheet metal forming processes by presenting a bending-dependent inverse isogeometric methodology," International Journal of Advanced Manufacturing Technology, **vol. 112**, no. 5-6, Jan. 2021, pp. 1389-1408

[13] *D.M. Neto, J. Coër, M.C. Oliveira*, "Numerical Analysis on The Elastic Deformation of The Tools in Sheet Metal Forming Processes," International Journal of Solids and Structures, **vol. 100-101**, no. 3, Dec. 2016, pp. 270-285

[14] *Ben-Elechi Slim, Khelifa Mourad, Bahloul Riadh*, "Sensitivity of friction coefficients, material constitutive laws and yield functions on the accuracy of springback prediction for an automotive part," International Journal of Material Forming, **vol. 14**, no. 2, Mar. 2021, pp. 323-340

[15] *Mohd, Ahmed*, "Adaptive Finite Element Simulation of Sheet Forming Process Parameters," Journal of King Saud University-Engineering Sciences, **vol. 30**, no. 3, Jul. 2018, pp. 259-265

[16] *D.M. Neto, M.C. Oliveira, A.D. Santos, J.L. Alves, L.F. Menezes*, "Influence of Boundary Conditions on The Prediction of Springback and Wrinkling in Sheet Metal Forming," International Journal of Mechanical Sciences, **vol. 122**, no. 5, Mar. 2017, pp. 244-254

[17] *Zheng Peng, Liu Dongliang, Guo Junke, Zhi Zhanxin*, "A new method for optimizing process parameters of active measurement grinding based on grey target decision making," Journal of Mechanical Engineering Science, **vol. 234**, no. 23, Dec. 2020, pp. 4645-4658

[18] *Hu Miao, Yang Zhiqiang , Cao Xiaolin, Yang Qing, Chen Yu, Li Xin*, "Study on Simulation of Stamping Forming and Die Surface Optimization of Aluminum Alloy Plate," Key Engineering Materials, **vol. 764**, no. 6, Feb. 2018, pp. 303–311

[19] *Li Gui, Liang Zhongkai*, "Intelligent design method and system of trimming block for stamping dies of complex automotive panels," International Journal of Advanced Manufacturing Technology, **vol. 109**, no. 9-12, Aug. 2020, pp. 2855–2897

[20] *Troive Lars, Bałon Paweł, Świątoniowski Andrzej, Mueller Thomas, Kiełbasa Bartłomiej*, "Springback compensation for a vehicle's steel body panel," International Journal of Computer Integrated Manufacturing, **vol. 31**, no. 2, Jul. 2018, pp. 152-163